

Shape Complementarity Optimization of Antibody-Antigen Interfaces: the Application to SARS-CoV-2 Spike Protein

Alfredo De Lauro ^{†,1} Lorenzo Di Rienzo ^{†,*,2} Mattia Miotto,² Pier Paolo Olimpieri,¹ Edoardo Milanetti,^{1,2} and Giancarlo Ruocco^{2,1}

¹*Department of Physics, Sapienza University, Piazzale Aldo Moro 5, 00185, Rome, Italy*

²*Center for Life Nano & Neuro-Science, Istituto Italiano di Tecnologia, Viale Regina Elena 291, 00161, Rome, Italy*

Biomolecules binding is influenced by many factors and its assessment constitutes a very hard challenge in computational structural biology. In this respect, the evaluation of shape complementarity at molecular interfaces is one of the key factors to be considered. Focusing on the peculiar case of antibody-antigen interaction, we designed a novel computational strategy based on in-silico mutagenesis of antibody binding site residues, where a Monte Carlo procedure aims at increasing the shape complementarity between the antibody paratope and a given epitope on a target protein surface. To quantify the complementarities occurring at the interface, we relied on a method we recently developed, which employs the 2D Zernike descriptors. To this end, we preliminarily considered an experimental structural dataset of antibody-antigen complexes, where our method statistically identifies, in terms of shape complementarity, pairs of interacting regions from non-interacting ones. We thus constructed our protocol against a molecular region in the N-terminal domain of SARS-CoV-2 Spike protein, already experimentally identified in interaction with antibodies in humans. We, therefore, optimized the shape of several possible template antibodies for the interaction with such a region. Lastly, we performed an independent molecular docking validation of the results of our protocol, thus evaluating also if the mutagenesis protocol introduced residues with chemical characteristics compatible with the target region.

I. INTRODUCTION

Cellular functioning is largely dependent on processes occurring when biological molecules recognize each other and bind [1, 2]. In particular, the non-covalent protein-protein pairing proved to be essential in several biochemical pathways, ranging from biocatalysis to organism immunity or cell regulatory network construction [3, 4]. Not surprisingly, in the last decades, a very high effort has been devoted to the development of computational tools for the structural characterization of protein-protein complexes. The aim of these methods are various, varying from binding site prediction [5, 6] to binding affinity prediction [7, 8] or protein-protein docking [9–12].

When the molecular compatibility between protein partners is studied, the understanding and quantification of the shape complementarity at the interface between them is one of the most basic tasks to solve [1]. Indeed, the evaluation of shape complementarity is essential for docking, both in terms of searching and evaluating the binding poses [2, 13–16], and represent one the factor to take into account for binding site recognition [5, 6] or to assess the binding affinity [17].

In this work, we focus on a specific and relevant class of proteins, namely antibodies.

Antibody-Antigen interaction, indeed, represents a very peculiar case of molecular recognition, whose interface shape complementarity level was shown to be

similar to the typical protein-protein interfaces [15, 18]. Moreover, the biomedical importance and the modular antibody architecture, that facilitates the engineering of novel antibody binding sites, in the past years made this class of molecules object of extensive studies [19–21].

Among the wide variety of methods developed in the last years, using the Zernike polynomials to describe the geometrical properties of a molecular region and to evaluate the complementarity with a putative binding partner region is an effective and promising strategy [22, 23]. Indeed, once extracted the portion of the molecular surface to be analyzed, its geometrical properties can be summarized through an ordered set of numerical descriptors, namely the Zernike descriptors, where the accuracy of the description can be indefinitely increased enlarging the number of descriptors considered [24–26].

It is worth noting that this representation is invariant if the surface is rotated, constituting therefore an absolute characterization of the examined protein region. Therefore the similarity and the complementarity between 2 molecular regions can be computed simply by comparing their Zernike descriptors, without the need of any preliminary superposition step [27, 28].

In the last decade, the Zernike approach, in its 3D version, has been widely applied for the analysis of biomolecules [22, 23, 27–34], proving its efficacy in characterizing both global and local proteins properties.

We recently developed a computational protocol that allows us to employ the 2D Zernike formalism to assess the shape complementarity observed in general in protein-protein interfaces and in particular in the interaction between SARS-CoV-2 Spike protein and its human cellular receptor, the angiotensin-converting enzyme 2 (ACE2) [6, 35–37]. The utilization of the 2D formal-

[†]These authors contributes equally to this work.

*Corresponding author:

lorenzo.dirienzo@iit.it

ism allows to sensibly decrease the computational time needed to compute the shape descriptors without significant loss in description accuracy [37].

Here, we collected a structural dataset of antibody-protein complexes solved in x-ray crystallography and we studied the interfaces shape complementarities through the application of our recently developed method based on 2D Zernike descriptors. We demonstrated that such a description can recognize with satisfying success the specific interaction from non-specific ones since paratopes show toward their corresponding epitopes a complementarity statistically higher than the ones computed when paratopes are compared with epitopes belonging to other antigens.

Based on these results, we propose a new computational protocol that, for a given target protein region, optimizes the shape complementarity of an antibody toward that region. Indeed, once a target region, belonging to a protein antigen, is identified and characterized with its Zernike descriptors, we compared that region with the paratope of the antibodies in our dataset. Selecting as starting template the most similar antibodies, we perform a Monte Carlo (MC) simulation for the optimization of the paratope: through extensive computational mutagenesis, substituting in each step an interacting antibody residue with a random one, we accept or reject each mutation according to the gain in shape complementarity, as evaluated by to Zernike descriptors.

Despite the generality of such an approach, we selected as a target for our protocol some surface region of SARS-CoV-2 Spike protein and we discuss here the results we got, given the high interest generated on such a protein by the urgency of the pandemic situation. In fact, the mechanisms of interaction between antibodies and Spike protein, as well as other viral membrane proteins, represent a key element for the design of new drugs and the development of new therapies.

II. RESULTS AND DISCUSSION

A. Description of Antibody-Antigen interface through Zernike Descriptors

In the present section, we discuss the results we obtained applying our recently developed computational protocol [6] on a structural dataset composed of 229 antibody-antigen complexes (See Methods).

In particular, we firstly identified for each complex the paratope (epitope) as the set of residues with at least one atom closer than 4 Å to any atom of the antigen (antibody). Therefore, after separately computing the Connolly surface [38] for both the proteins in interaction, we extracted the portions of the molecular surfaces relating to the residues of the binding site, to properly characterize the shape of the interacting regions of antibodies and antigens (See Figure 1.A).

Once identified the interacting regions, we character-

ized them through invariant 2D Zernike polynomials, summarizing their geometrical properties in an ordered set of numerical descriptors. Since two perfectly fitting surfaces are characterized by the same shape, the difference between their Zernike descriptors is, in principle, equal to zero. Therefore, this compact representation allows an easy assessment of the shape complementarity between the two molecular regions: indeed, the lower is the distance between the Zernike descriptors, the higher is the shape complementarity between the corresponding protein regions [6, 37].

After that all the paratopes and epitopes in the dataset have been described through the Zernike formalism, we defined the *specific complementarities* as the distances computed between interacting paratope-epitope pairs and the *non-specific complementarities* as the distances computed when 2 regions belonging to different complexes are compared. In other words, dealing with N antibody-antigen complexes, the specific complementarity, C_s , is defined as:

$$D(p_i, e_j)|_{i=j} = \sqrt{\sum_{k=1}^{121} (p_i^k - e_j^k)^2 |_{i=j}} \quad (1)$$

where D is basically the Euclidean distance between the vectors of the paratope (p_i) and epitope (e_i) Zernike descriptors. Since we expanded all the paratopes and epitopes to order 20, we dealt with 121 descriptors for each binding region. On the other hand, the non-specific complementarities, C_{ns} , can be computed as:

$$D(p_i, e_j)|_{i \neq j} = \sqrt{\sum_{k=1}^{121} (p_i^k - e_j^k)^2 |_{i \neq j}} \quad (2)$$

In Figure 1.B we reported a boxplot highlighting the differences between C_s and C_{ns} . As expected, the distribution of C_s is statistically lower than the distribution of C_{ns} (Kolmogorov-Smirnov test p-value $< 2.2e - 16$), testifying the sensitivity of Zernike in recognizing regions actually in interaction from random ones.

To further test this sensitivity we normalized the Zernike complementarities with the Z-score. In particular, for each paratope we have 1 C_s and 228 C_{ns} complementarities. Normalizing over this set of numbers and looking at the Z-score regarding the specific interaction, we assessed the propensity that characterizes each antibody toward its specific antigen. In Figure 1.C we report the distribution of such specific Z-scores: as evident, they are mostly negatives (86% of the cases have Z-score lower than 0, 28% have Z-score lower than -1), providing evidence that specific interactions are basically characterized by lower distances (higher complementarity) than non-specific ones.

Taken together, these results confirm the ability of our method to correctly capture the main determinant of molecular shape complementarity.

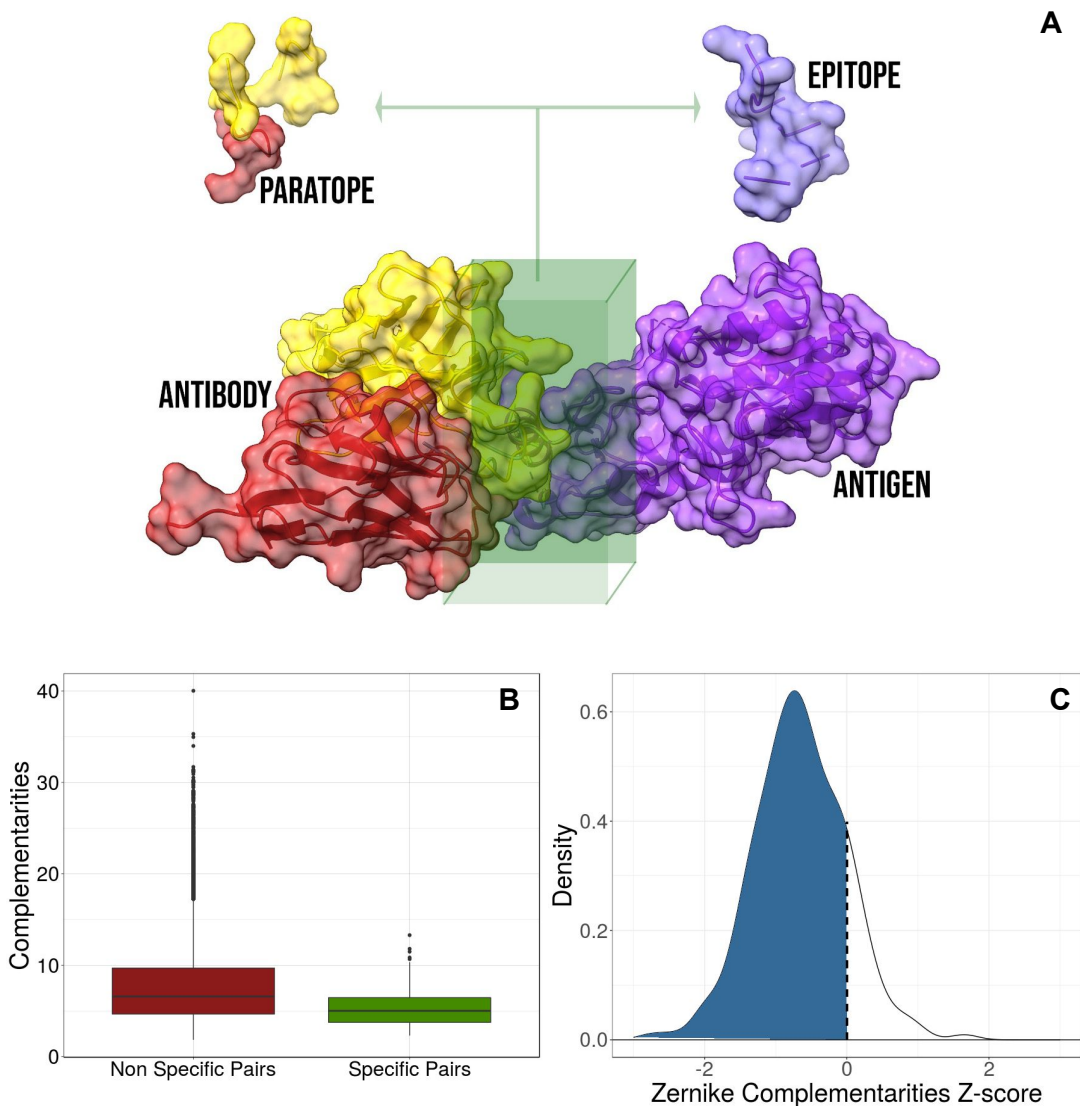


FIG. 1: **Application of the 2D Zernike polynomials approach to antibody-antigen complexes.** **A)** Representation of a generic molecular antibody-antigen complex: the antibody heavy chain, antibody light chain, and the antigen are in red, yellow, and purple, respectively. The interacting regions, defined as the portion of the molecular surfaces belonging to residues closer than 4 \AA to any atoms of the molecular partner, are extracted from the whole surface. **B)** Boxplot comparing the *specific complementarity*, i.e. the complementarity between regions actually found in interaction (green), and the *non-specific complementarity*, i.e. the complementarity observed between paratopes and epitopes of different complexes (red). It is worth remarking that when the numerical value is low, the complementarity is high. **C)** Z-scores distribution of the specific complementarity. When the Z-score is lower than 0, the specific interaction is characterized by a complementarity higher than the mean of the non-specific interaction.

B. Monte Carlo Method for optimization of molecular interface

The Zernike formalism enjoys several advantageous features in represent molecular surface: mainly, the invariance under rotation that makes such descriptors an “absolute” characterization of local protein morphology and the low computational cost of its calculation. Indeed, in this section we present our algorithm that, exploiting these advantages, aims to the optimization of shape com-

plementarity toward a given molecular target region.

The main steps of the protocol are depicted in Figure 2.A. Once identified the target region, i.e. the portion of protein molecular surface to which an antibody will be optimized, it is necessary to identify the starting point of the algorithm. Indeed, summarized with the Zernike descriptors the target region we can compute the shape complementarity with all the paratope of our dataset: here, the template, i.e. the antibody selected as the starting point for the mutagenesis process, can be cho-

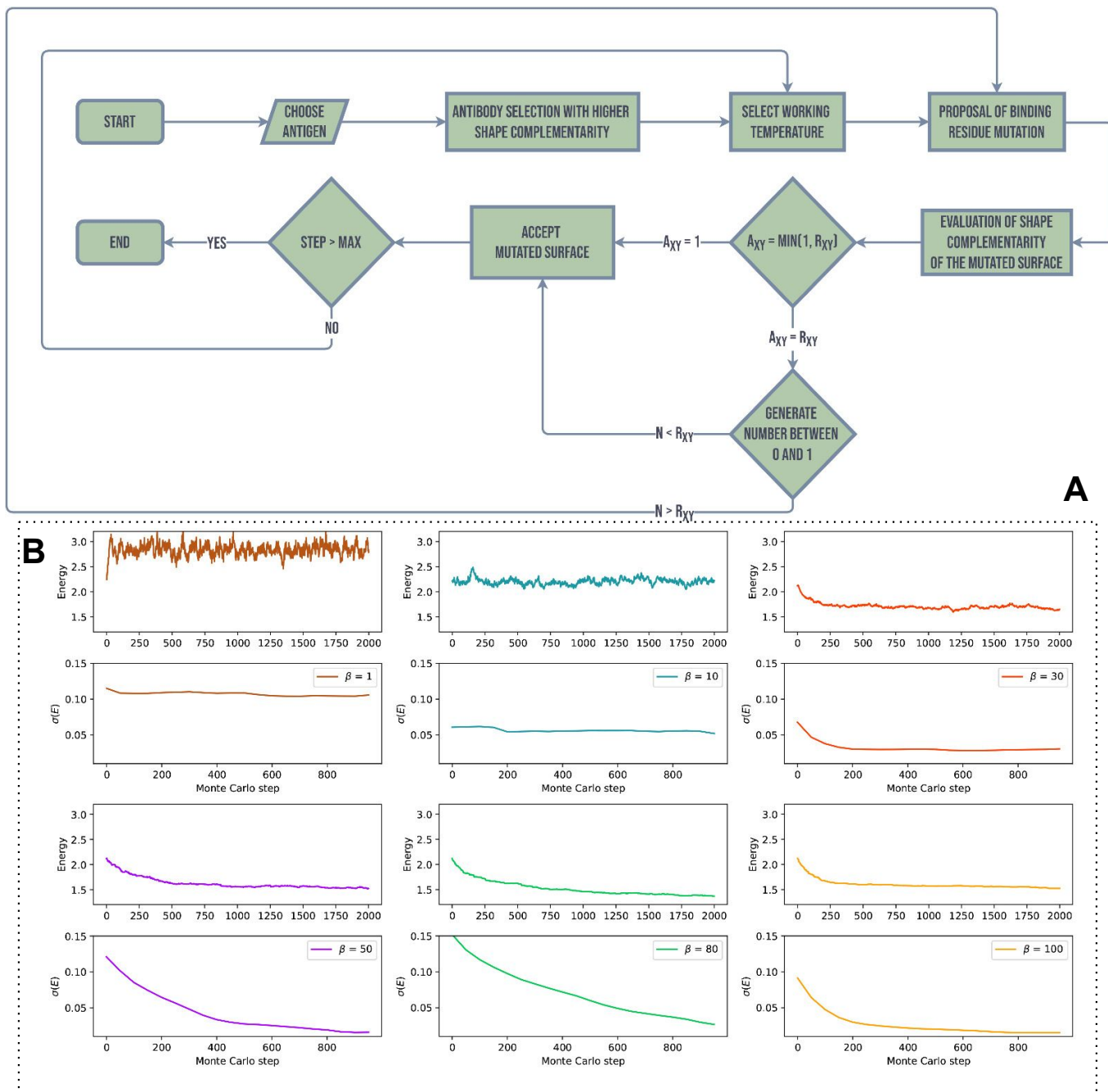


FIG. 2: **Development of a Monte Carlo for shape complementarity optimization against a target region. A)** Flowchart depicting the main steps of the computational protocol we developed. **B)** Results of the mutagenesis Monte Carlo procedures performed at fixed β ($\beta = 1, 10, 30, 50, 80, 100$). The top panels represent the energy (i.e. the shape complementarity) as a function of the Monte Carlo steps. The low panels show the standard deviation of energy of the remaining part of the Monte Carlo simulations as a function of the Montecarlo steps (i.e. $\sigma(E)$ for $n = 1000$ means standard deviations of the energy obtained in the steps 1001-2000).

sen among the paratopes characterized by a high initial complementarity.

Established the template, and therefore the initial molecular region with a given complementarity with the epitope, we performed a Monte Carlo simulation employ-

ing computational mutagenesis on the paratope residues. Indeed, in each step, we randomly selected and mutated a residue in another of the 19 possible ones. The mutation generates a new paratope, characterized by a different shape of its molecular surface. Consequently, recomput-

ing the Zernike descriptors we can evaluate the effect of the mutation on the complementarity with the target region: indeed we can define the *complementarity balance* as:

$$\Delta C = C_{mut} - C_{wt} = D(p_{mut}, e_{tar}) - D(p_{orig}, e_{tar}) \quad (3)$$

where p_{orig} and p_{mut} are the Zernike descriptors of the original and the mutated paratope respectively, while the e_{tar} represent the Zernike descriptors of the target epitope and D represent the distance between 2 sets of descriptors. Since, as said, a high complementarity is reached when D is low, $\Delta C < 0$ means a higher complementary surface, and $\Delta C > 0$ is obtained when the mutation is deleterious, since it causes a worsening of the shape complementarity.

The number of combinations of possible mutations in an interacting region, composed usually of tens of residues, is huge. Therefore, to effectively sample the space of the possible mutants, we perform a Monte Carlo Metropolis simulation, iterating the procedure described above, where the mutation in each step is accepted according to the following rules:

$$P = \begin{cases} 1 & \text{if } \Delta C < 0 \\ e^{-\beta\Delta C} & \text{if } \Delta C \geq 0 \end{cases} \quad (4)$$

where β is the temperature factor that determines the probability of acceptance of a step worsening complementarity. Note that this aspect is crucial to properly explore a large number of different mutants: β is thus progressively decreased during the Monte Carlo simulation, progressively confining the system in an energy minimum in a simulated annealing process [39].

To observe how many steps are necessary to reach the equilibrium for each β , we preliminary ran several fixed-temperature Monte Carlo simulations. Indeed, we selected the epitope of an antigen structure in our dataset (PDB id: 1AR1) and, excluding its own one, we choose as the starting template the most complementary paratope in the structural dataset. We thus performed six different Monte Carlo simulations, each for a different β , where the acceptance probability in each mutagenesis step is given by Eq. 4. Performing 10 independent simulations of $N = 2000$ steps for each β , the averaged results we obtained are summarized in Figure 2.B. In the top panels, we reported the energy (i.e. the complementarity) as a function of the Monte Carlo steps. In the low panels, we reported the standard deviation of the energy of the remaining part of the Monte Carlo simulations as a function of the Montecarlo steps (i.e. $\sigma(E)$ for $n = 1000$ means standard deviations of the energy obtained in the steps 1001-2000). As expected, for low values of β (i.e. high temperature) the system lives in a condition of indifferent equilibrium, where whatever mutation have equal likelihood to be accepted, independently from its effect on complementarity. When, on the contrary, β is high,

the energy of the system rapidly decreases to a stationary local minimum. This trend is confirmed by looking at the stationary value of energies or, equivalently, noting that standard deviation tends progressively to 0. In the light of these results, in our protocol, we set $N = 700$ for each temperature. In this way, we preliminary allow the system to move away from the starting local conformation, thus freezing it in a new energy minimum, characterized by an increased shape complementarity with the target region.

C. A Case of Study: Application to SARS-CoV-2 Spike Protein

Despite the generality of the approach here described, we applied it to a very relevant and urgent case of macromolecular interaction. Indeed, the severe acute respiratory syndrome coronavirus 2 (SARS-CoV-2) infection, caused by the human infection of a new coronavirus, is causing very serious danger for public health [40, 41].

Therapeutic strategies are mainly devoted to SARS-CoV-2 Spike protein, protruding from the viral envelope and responsible for cell entry mechanism [42–44]. In this framework, it has been recently revealed the structural details of a neutralizing antibody bound to the N-terminal domain of Spike protein [45], identifying a promising molecular target for the design of therapeutic drugs against COVID-19: therefore, we decided to test our protocol optimizing antibodies targeting such an epitope (See Figure 3).

Selected the epitope residues on the Spike N-terminal domain and characterized their molecular surface through Zernike formalism, we calculated the complementarity between this epitope and all the antibody binding sites in our dataset. The distribution of the complementarities observed is reported in Figure 3.A: in order to begin the optimization from a favorite starting point, we selected as templates antibody binding sites characterized by a high complementarity with the identified target. Indeed, looking at the distribution of non-specific complementarities (Eq. 2), we identified the threshold value delimiting the 5% with most complementarity.

We selected an antibody binding site as a template if such Zernike distance is lower than 3.29 (dashed line in Figure 3.A), the upper bound of the 5% lower interval of the distribution of non-specific complementarities (Eq. 2). This meaning that the independent simulations we ran started from antibodies characterized by a probability lower than 5% that the observed shape complementarity belongs to the distributions of non-specific interaction. We therefore selected as starting point six different antibody binding sites (PDB ids: 1EGJ, 2YBR, 4AG4, 3Q1S, 3UYP, 4G3Y), giving us the possibility to analyze the stability of the results deriving from six independent simulations.

We, therefore, applied the procedure described in the

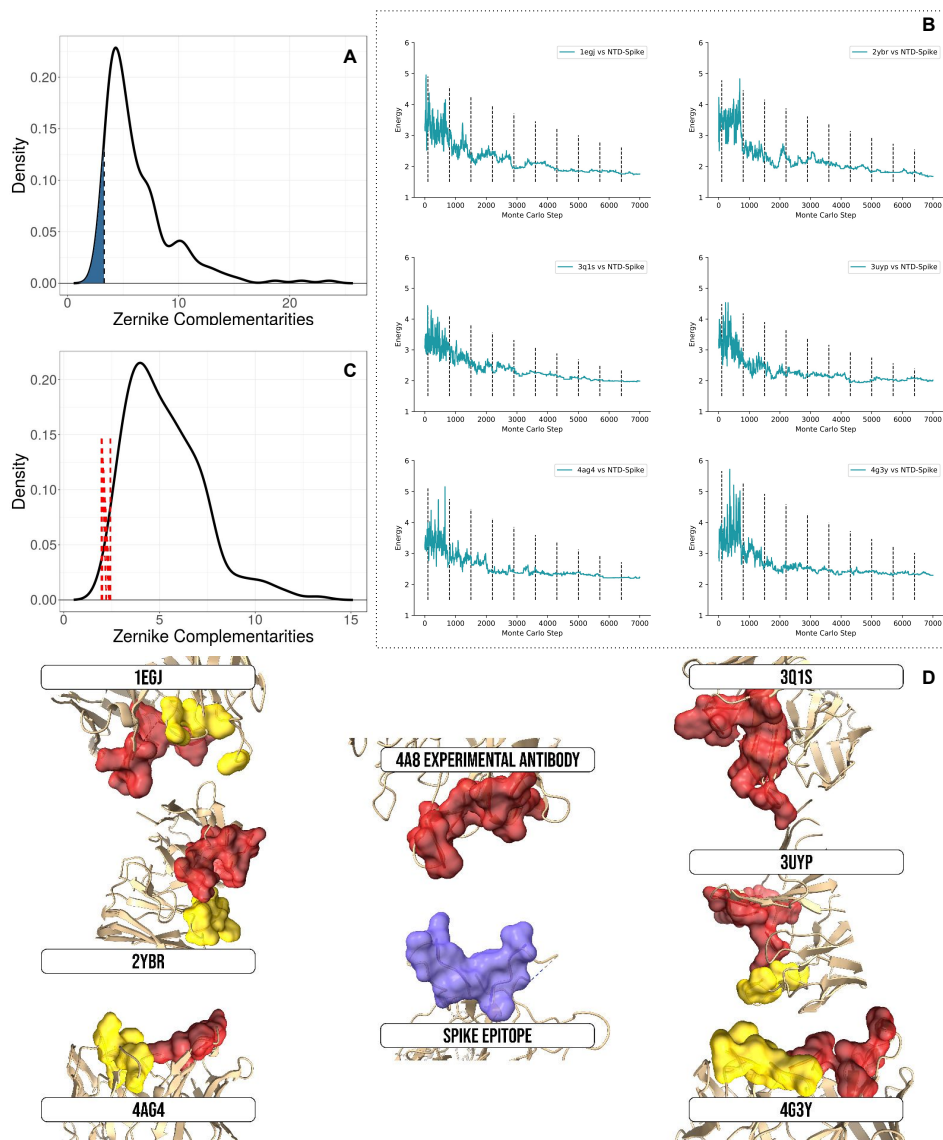


FIG. 3: Application of the optimization protocol to SARS-CoV-2 Spike protein. **A)** Distribution of the complementarities between the epitope in the N-terminal domain and the paratopes of our structural dataset. The dashed line represents the upper bound of the 5% lower interval of the distribution of non-specific complementarities (Eq. 2). We selected as starting template for optimization procedure the antibodies characterized by an initial shape complementarity lower than such value, in order to begin from a favorite starting point. **B)** Shape complementarity as a function of the Monte Carlo steps for all the antibodies we optimized. Dashed lines separate different temperature intervals of the simulations. **C)** Distributions of the specific complementarities (Eq. 1) observed in our structural dataset. Red dashed lines represent the shape complementarities we get at the end of our optimization procedure. **D)** Molecular representation of the experimental antibody binding an epitope in Spike N-terminal domain (in the center). In the lateral figures, we reported the paratopes optimized for matching such epitope, labeled with the PDB code of their template antibody.

previous section. In Figure 3.B, we reported, for each of the Monte Carlo simulations performed, the shape complementarity as a function of the steps of the simulation, where the dashed lines enclose ranges with different β values. Each simulation significantly optimizes shape complementarity, obtaining a Zernike distance decrease of 26%, on average. Significantly, all the designed binding sites are characterized by a very high final shape complementarity: indeed, if we look at the distribution of

specific complementarities (Eq. 1) in Figure 3.C, it is notable that all the designed binding site is in the 2% left tail of such distribution (orange dashed lines). The optimization of shape complementarity is confirmed also by looking at the molecular images shown in Figure 3.D, where both the experimental and the designed interacting surfaces are reported. As it can be noted, the morphology of the experimental paratope - characterized by a central depression surrounded by 2 protruding parts -

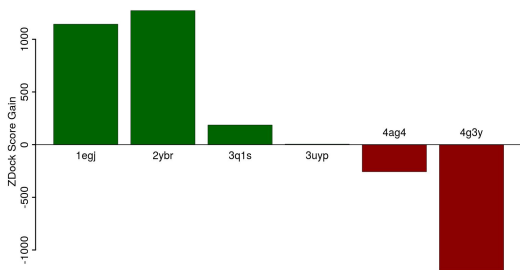


FIG. 4: **Results of the docking analysis.** Each bar represents the difference between the best scores we obtained using original and optimized antibodies. When the values are higher than 0, the computational protocol we applied increased the docking compatibility (green bars); conversely, when the values are lower than 0 the docking score is decreased after shape complementarity optimization (red bars). We assumed a score of 0 when ZDOCK can not find docking poses satisfying the required constraints.

was overall acquired also by all the designed paratopes.

Lastly, to further verify the goodness of the proposed mutant, not only in terms of shape complementarity optimization but also in terms of other important binding properties such as electrostatic or hydrophobicity, antibodies we performed a molecular docking analysis using ZDOCK method [46], which is one of the state-of-the-art methods. In particular, we docked Spike protein and the antibodies, both in the original and in the designed structure through the optimization of the only shape complementarity, to study the improvement our computational protocol has brought about. Constraining the interacting region to the residues composing the Spike target epitope and the antibodies optimized regions, we summarized in Figure 4 the results we obtained. We report the difference between the best scores we obtained using original and optimized antibodies (when the values are higher than 0 the optimization increases the docking compatibility, and we assume a score of 0 where ZDOCK can not find docking poses satisfying the required constraints).

It is worth remarking that in our procedure we do not consider important factors that dramatically affect the biomolecules compatibility, such as electrostatics or hydration properties. This notwithstanding, it can be noted that in some cases the optimization of shape has the effect of improving the docking score, probably because we do not select residues characterized by unfavorable chemical characteristics. Therefore, this allows us to verify in which types of binding shape complementarity plays a predominant role. In this specific case, only two cases out of 4 do not show a significant improvement in the docking evaluation score.

III. CONCLUSIONS

The binding affinity between biomolecules is the result of a complex balance of several effects, including enthalpic and entropic contributions. Indeed, the substitution of even one residue at the interface could produce dramatic changes: although many efforts were spent in this direction, predicting such effects has proven to be a difficult task and is still an open problem in computational biology.

In this scenario, the evaluation of shape complementarity between molecular regions is undoubtedly a basic and important factor to be evaluated, which is a condition often necessary but not sufficient to evaluate the goodness of the binding. In this work, we focused on a relevant case of molecular recognition, antibody-antigen interaction, and we applied our recently developed formalism based on the 2D Zernike polynomials in order to evaluate the shape complementarity with a quantitative approach. Once summarized the topological properties of interacting regions with a set of numerical descriptors, we demonstrated that such formalism assigns to pairs of interacting regions complementarities statistically higher than the ones assigned to regions not in interaction.

Using these results, we developed a Monte Carlo approach for the shape optimization of an antibody towards a molecular target region, proposing a new strategy which, potentially, can propose the antibody with the highest shape complementarity for a given region of the molecular surface of any antigen protein.

Also because of the emergence of viral variants that can eventually escape antibodies matured in vaccinated or recovered patients, the interactions between antibodies and SARS-CoV-2 Spike protein are being extensively studied and still needs further investigation.

For this reason, we selected a molecular region in the Spike N-terminal domain, already identified as a possible epitope for antigen recognition, as the target region for our procedure. We, therefore, devised a set of antibodies characterized by a high shape complementarity toward that epitope. It is important to note that, even in this work we do not consider other factors important to optimize binding between biomolecules, such as electrostatics or hydrophobicity, an independent molecular docking evaluation testifies that in many cases the optimization procedure increases the obtained docking scores.

Including in the Monte Carlo cost function terms accounting for other aspects of binding compatibility, this procedure can represent a promising strategy for interface region molecular design.

IV. MATERIALS AND METHODS

A. Dataset

We selected 229 protein-binding antibodies with sequence identity lower than 90% and resolution $< 3.0 \text{ \AA}$

using the SabDab database [47]. The sequence of each antibody was renumbered according to the Chothia numbering scheme [48, 49] using an in-house python script.

The structure of the molecular complex between SARS-CoV-2 Spike protein and the human antibody 4A8 is labeled with the PDB code 7C2L.

B. Surface Construction

Using as reference the experimental structures, computational mutagenesis has been performed using SCWRL4 [50].

For each protein structure, Solvent Accessible Surface is computed using DMS software with standard option [38]. The interacting surface is constituted by the surface points belonging to interacting residues, defined as the set of residues having at least one atom closer than 4 Å to any atoms of the molecular partner.

C. Zernike Descriptors

Given a 2D function $f(r, \phi)$ in the unitary circle (region $r < 1$), it can be expanded in the Zernike polynomials basis. Therefore:

$$f(r, \phi) = \sum_{n=0}^{\infty} \sum_{m=0}^{m=n} c_{nm} Z_{nm} \quad (5)$$

where

$$\begin{aligned} c_{nm} &= \frac{(n+1)}{\pi} \langle Z_{nm} | f \rangle = \\ &= \frac{(n+1)}{\pi} \int_0^1 dr r \int_0^{2\pi} d\phi Z_{nm}^*(r, \phi) f(r, \phi) \end{aligned} \quad (6)$$

are the expansion coefficients (Zernike moments). The

complex functions $Z_{nm}(r, \phi)$ are the Zernike polynomials, each composed by a radial and an angular part:

$$Z_{nm} = R_{nm}(r) e^{im\phi}. \quad (7)$$

The radial dependence, given n and m , can be written as follow:

$$R_{nm}(r) = \sum_{k=0}^{\frac{n-m}{2}} \frac{(-1)^k (n-k)!}{k! \left(\frac{n+m}{2} - k\right)! \left(\frac{n-m}{2} - k\right)!} r^{n-2k} \quad (8)$$

For each couple of polynomials, this rule holds:

$$\langle Z_{nm} | Z_{n'm'} \rangle = \frac{\pi}{(n+1)} \delta_{nn'} \delta_{mm'} \quad (9)$$

Therefore the set of polynomials forms a basis. Knowing the coefficients, $\{c_{nm}\}$ allows the reconstruction of the original function. The level of the detail can be modified by modulating the order of expansion, $N = \max(n)$.

The norm of each coefficient ($z_{nm} = |c_{nm}|$) does not depend on the phase, therefore it is invariant under rotations around the origin.

The shape complementarity between two regions can be evaluated by comparing their Zernike invariants. In particular, we measured the complementarity between region i and j as the Euclidean distance between the invariant vectors, i.e.

$$d_{ij} = \sqrt{\sum_{k=1}^{M=121} (z_i^k - z_j^k)^2} \quad (10)$$

We adopted $N=20$, therefore dealing with 121 invariant descriptors for each patch.

-
- [1] S. Jones and J. M. Thornton, Proceedings of the National Academy of Sciences **93**, 13 (1996).
- [2] M. M. Gromiha, K. Yugandhar, and S. Jemimah, Current opinion in structural biology **44**, 31 (2017).
- [3] A.-C. Gavin, M. Börsche, R. Krause, P. Grandi, M. Marzioch, A. Bauer, J. Schultz, J. M. Rick, A.-M. Michon, C.-M. Cruciat, et al., Nature **415**, 141 (2002).
- [4] J.-D. J. Han, N. Bertin, T. Hao, D. S. Goldberg, G. F. Berriz, L. V. Zhang, D. Dupuy, A. J. Walhout, M. E. Cusick, F. P. Roth, et al., Nature **430**, 88 (2004).
- [5] P. Gainza, F. Sverrisson, F. Monti, E. Rodola, D. Boscaini, M. Bronstein, and B. Correia, Nature Methods **17**, 184 (2020).
- [6] E. Milanetti, M. Miotto, L. Di Rienzo, M. Monti, G. Gosti, and G. Ruocco, Computational and structural biotechnology journal **19**, 29 (2021).
- [7] T. Siebenmorgen and M. Zacharias, Wiley Interdisciplinary Reviews: Computational Molecular Science **10**, e1448 (2020).
- [8] A. Vangone and A. M. Bonvin, elife **4**, e07454 (2015).
- [9] I. A. Vakser, Biophysical journal **107**, 1785 (2014).
- [10] D. Kozakov, D. R. Hall, B. Xia, K. A. Porter, D. Padhorny, C. Yueh, D. Beglov, and S. Vajda, Nature protocols **12**, 255 (2017).
- [11] C. Geng, Y. Jung, N. Renaud, V. Honavar, A. M. Bonvin, and L. C. Xue, Bioinformatics **36**, 112 (2020).
- [12] Y. Yan, H. Tao, J. He, and S.-Y. Huang, Nature protocols **15**, 1829 (2020).
- [13] R. Chen and Z. Weng, Proteins: Structure, Function, and Bioinformatics **51**, 397 (2003).

- [14] G. Nicola and I. A. Vakser, *Bioinformatics* **23**, 789 (2007).
- [15] D. Kuroda and J. J. Gray, *Bioinformatics* **32**, 2451 (2016).
- [16] Y. Yan and S.-Y. Huang, *BMC bioinformatics* **20**, 1 (2019).
- [17] A. Erijman, E. Rosenthal, and J. M. Shifman, *PLOS one* **9**, e110085 (2014).
- [18] Y. Li, H. Li, F. Yang, S. J. Smith-Gill, and R. A. Mariuzza, *Nature Structural & Molecular Biology* **10**, 482 (2003).
- [19] S. Singh, N. K. Tank, P. Dwiwedi, J. Charan, R. Kaur, P. Sidhu, and V. K. Chugh, *Current clinical pharmacology* **13**, 85 (2018).
- [20] A. F. Saeed, R. Wang, S. Ling, and S. Wang, *Frontiers in microbiology* **8**, 495 (2017).
- [21] P. Gotwals, S. Cameron, D. Cipolletta, V. Cremasco, A. Crystal, B. Hewes, B. Mueller, S. Quarantino, C. Sabatos-Peyton, L. Petruzzelli, et al., *Nature Reviews Cancer* **17**, 286 (2017).
- [22] V. Venkatraman, L. Sael, and D. Kihara, *Cell biochemistry and biophysics* **54**, 23 (2009).
- [23] L. Di Rienzo, E. Milanetti, R. Lepore, P. P. Olimpieri, and A. Tramontano, *Scientific reports* **7**, 1 (2017).
- [24] F. Zernike, *Monthly Notices of the Royal Astronomical Society* **94**, 377 (1934).
- [25] M. Novotni and R. Klein, *Computer-Aided Design* **36**, 1047 (2004).
- [26] N. Canterakis, in *In 11th Scandinavian Conf. on Image Analysis* (Citeseer, 1999).
- [27] S. Daberdaku and C. Ferrari, *BMC bioinformatics* **19**, 35 (2018).
- [28] L. Di Rienzo, E. Milanetti, J. Alba, and M. D’Abramo, *Journal of Chemical Information and Modeling* **60**, 1390 (2020).
- [29] V. Venkatraman, Y. D. Yang, L. Sael, and D. Kihara, *BMC bioinformatics* **10**, 407 (2009).
- [30] D. Kihara, L. Sael, R. Chikhi, and J. Esquivel-Rodriguez, *Current Protein and Peptide Science* **12**, 520 (2011).
- [31] J. Alba, L. Di Rienzo, E. Milanetti, O. Acuto, and M. D’Abramo, *Cells* **9**, 942 (2020).
- [32] S. Daberdaku and C. Ferrari, *Bioinformatics* **35**, 1870 (2019).
- [33] X. Han, A. Sit, C. Christoffer, S. Chen, and D. Kihara, *PLoS computational biology* **15**, e1006969 (2019).
- [34] L. Di Rienzo, E. Milanetti, C. Testi, L. C. Montemiglio, P. Baiocco, A. Boffi, and G. Ruocco, *Computational and structural biotechnology journal* **18**, 2678 (2020).
- [35] E. Milanetti, M. Miotto, L. D. Rienzo, M. Nagaraj, M. Monti, T. W. Golbek, G. Gosti, S. J. Roeters, T. Weidner, D. E. Otzen, et al., *Frontiers in Molecular Biosciences* **8** (2021).
- [36] M. Miotto, L. D. Rienzo, L. Bò, A. Boffi, G. Ruocco, and E. Milanetti, *Frontiers in Molecular Biosciences* **8** (2021).
- [37] L. Di Rienzo, M. Monti, E. Milanetti, M. Miotto, A. Boffi, G. G. Tartaglia, and G. Ruocco, *Computational and Structural Biotechnology Journal* (2021).
- [38] F. M. Richards, *Annual review of biophysics and bioengineering* **6**, 151 (1977).
- [39] S. Kirkpatrick, C. D. Gelatt, and M. P. Vecchi, *science* **220**, 671 (1983).
- [40] C. Huang, Y. Wang, X. Li, L. Ren, J. Zhao, Y. Hu, L. Zhang, G. Fan, J. Xu, X. Gu, et al., *The Lancet* **395**, 497 (2020).
- [41] N. Zhu, D. Zhang, W. Wang, X. Li, B. Yang, J. Song, X. Zhao, B. Huang, W. Shi, R. Lu, et al., *New England Journal of Medicine* (2020).
- [42] P. Zhou, X.-L. Yang, X.-G. Wang, B. Hu, L. Zhang, W. Zhang, H.-R. Si, Y. Zhu, B. Li, C.-L. Huang, et al., *Nature* pp. 1–4 (2020).
- [43] A. C. Walls, Y.-J. Park, M. A. Tortorici, A. Wall, A. T. McGuire, and D. Veasley, *Cell* (2020).
- [44] Y. Wan, J. Shang, R. Graham, R. S. Baric, and F. Li, *Journal of virology* (2020).
- [45] X. Chi, R. Yan, J. Zhang, G. Zhang, Y. Zhang, M. Hao, Z. Zhang, P. Fan, Y. Dong, Y. Yang, et al., *Science* **369**, 650 (2020).
- [46] B. G. Pierce, K. Wiehe, H. Hwang, B.-H. Kim, T. Vreven, and Z. Weng, *Bioinformatics* **30**, 1771 (2014).
- [47] J. Dunbar, K. Krawczyk, J. Leem, T. Baker, A. Fuchs, G. Georges, J. Shi, and C. M. Deane, *Nucleic acids research* **42**, D1140 (2013).
- [48] C. Chothia and A. M. Lesk, *Journal of molecular biology* **196**, 901 (1987).
- [49] C. Chothia, A. M. Lesk, A. Tramontano, M. Levitt, S. J. Smith-Gill, G. Air, S. Sheriff, E. A. Padlan, D. Davies, W. R. Tulip, et al., *Nature* **342**, 877 (1989).
- [50] G. G. Krivov, M. V. Shapovalov, and R. L. Dunbrack Jr, *Proteins: Structure, Function, and Bioinformatics* **77**, 778 (2009).